Generation of squeezed microwave states by a dc-pumped degenerate parametric Josephson junction oscillator

Franz X. Kaertner and Peter Russer
Institut für Hochfrequenztechnik, Technische Universität München, Arcisstrasse 21, D-8000 München 2, Federal Republic of Germany
(Received 30 May 1990)

The master equation for a dc-pumped degenerate Josephson parametric amplifier is derived. It is shown that the Wigner distribution representation of this master equation can be approximated by a Fokker-Planck equation. By using this equation, the dynamical behavior of this degenerate Josephson amplifier with respect to squeezing of the radiation field is investigated. It is shown that below threshold of parametric oscillation, a squeezed vacuum state can be generated, and above threshold a second bifurcation point exists, where the device generates amplitude squeezed radiation. Basic relations between the achievable amplitude squeezing, the output power, and the operation frequency are derived.

I. INTRODUCTION

Squeezed states of the radiation field can be used in several ways to increase the sensitivity of precision measurements. One way can, in principle, be described as a substitution of the conventionally vacuum fluctuations by squeezed vacuum fluctuations. Thus the fluctuations inevitably coupled to the system by the dissipation fluctuation theorem are modified in such a way that they do not degrade the sensitivity of the measurement. See, for example, the method of back-action evasion[1] and high-resolution interferometry.[2] For these applications one has to produce a squeezed vacuum state. That means a squeezed state with vanishing averages for the in-phase and quadrature components.

Another application of squeezed states for high-precision measurement is in homodyne and heterodyne detection, when the signal field to be detected is strong, or the available local oscillator power cannot be chosen high enough. In this case one can make use of a local oscillator emitting a squeezed state with nonvanishing amplitude but reduced amplitude fluctuations to improve the signal-to-noise ratio in the detection signal.[3,4] Squeezed states with and without an average amplitude may be used in realizing Shapiro's lossless tap situation.[5]

In this paper we will investigate the possibility of generating such squeezed states by a dc-pumped degenerate Josephson parametric amplifier (DCPJPA). In Ref. 6 we have shown that below threshold of oscillation the DCPJPA can be used to generate squeezed vacuum states, and as is well known, the squeezing of a parametric amplifier reaches a maximum when it is operated at the threshold for parametric oscillation.[7] Above this threshold the signal emitted by the parametric oscillator has a nonvanishing amplitude and the fluctuations in the quadrature and in-phase component of the signal may also be squeezed as is known from the optical parametric oscillator.[8] For an analysis of the properties of these states of the radiation field created by the DCPJPA we have to start with the nonlinear quantum Langevin equations for this device derived in Ref. 6. In Sec. II we derive the master equation governing the behavior of the DCPJPA. From the master equation for the density operator we can derive the evolution equation of the corresponding Wigner distribution. Under certain conditions this evolution equation approaches a classical Fokker-Planck equation. In Sec. III we will discuss the stationary points of this equation and the stability of these points; this gives an overview of the dynamical behavior of this device. The properties of the system with respect to squeezing of the cavity mode and the output field will be calculated in Sec. IV. This will be done by a semiclassical input-output formalism introduced by Reynaud and Heidmann.[9] Finally in Sec. V we will calculate the output power of the oscillator and the frequency range where squeezed radiation can be generated.

II. THE MASTER EQUATION OF THE DCPJPA

A schematic circuit diagram of the DCPJPA is shown in Fig. 1.[6] It shows a Josephson junction, which is modeled by the resistively shunted junction model (RSJ), coupled via a dc-voltage source to a resonator, modeled by a parallel resonant circuit. The shunt resistance R of the Josephson junction is modeled as the transmission line to the left with characteristic impedance R.[10] By the transmission line to the right the signal generated by the device may be coupled to a detector to investigate the

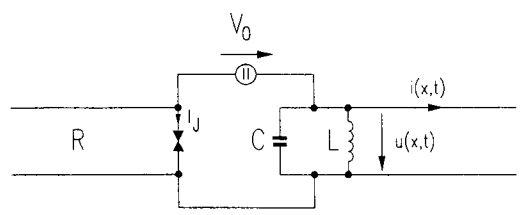

FIG. 1. Schematic circuit diagram of the DCPJPA.

properties of the emitted radiation or to use it in an experimental setup. As was rigorously derived in Ref. 6, in the rotating-wave approximation the quantum-dynamical behavior of the DCPJPA is governed by the following quantum Langevin equation:

$$\frac{da}{dt}=-\frac{\gamma}{2}a-\frac{i}{\hbar}[a,\bar{H}_{\rm sys}(a,a^\dagger)] -(\gamma_R)^{1/2}a_R^{\rm in}(t)-(\gamma_S)^{1/2}a_S^{\rm in}(t)\ , \tag{1}$$

where $a^\dagger$ and a are the creation and annihilation operators of the cavity mode with frequency Ω. The Hamiltonian $\bar{H}_{\rm sys}(a,a^\dagger)$ is the Hamiltonian of the dc-pumped Josephson junction averaged over one period of oscillation $T=2\pi\Omega$:

$$\bar{H}_{\rm sys}(a,a^\dagger)=\frac{1}{T}\int_0^T E_J\{1-\cos[\omega_0 t-\varphi_0 +\kappa(ae^{-i\Omega t}+a^\dagger e^{i\Omega t})]\}dt\ . \tag{2}$$

The frequency

$$\omega_0=\frac{2e_0}{\hbar}V_0 \tag{3}$$

is the pump frequency of the Josephson junction due to the applied dc voltage. The phase $\varphi_0=(2e_0L/\hbar R)V_0$ is 2π times the number of magnetic flux quanta $\Phi_0=h/2e_0$ stored in the inductance L due to the dc current caused by the dc-voltage source V_0 and flowing through L over the shunt resistance R of the Josephson junction. The constant

$$\kappa=(2e_0^2/\hbar\Omega C)^{1/2} \tag{4}$$

is a measure for the strength of the coupling of the cavity field to the Josephson junction. The dimensionless ratio κ/π is the average number of flux quanta, stored in the inductance L, per photon excited in the cavity mode, and

$$E_J=\frac{\hbar I_c}{2e_0} \tag{5}$$

is the coupling energy of the Josephson junction, where I_c is the critical current of the junction. Due to the coupling of the Josephson junction to the signal transmission line and the shunt resistance R the energy radiated into these subsystems leads to a damped motion of the cavity mode with the total loss rate $\gamma=\gamma_S+\gamma_R$ where the loss rates γ_S and γ_R due to the signal transmission line and the shunt resistance, respectively, are given by

$$\gamma_S=\frac{1}{R_SC}\quad\text{and}\quad\gamma_R=\frac{1}{RC}\ . \tag{6}$$

According to the dissipation fluctuation theorem these loss mechanisms give rise to fluctuations described by the input-field operators $a_{S/R}^{\rm in}(\omega)$ of the inward traveling flux waves of frequency ω of the transmission lines[6] by

$$a_{S/R}^{\rm in}(t)=\frac{1}{\sqrt{2\pi}}\int_{-\infty}^{+\infty}\hat{a}_{S/R}^{\rm in}(\Omega+\omega)e^{-i\omega t}d\omega\ . \tag{7}$$

The output field onto the signal transmission line is related to the input field and the cavity mode according to

$$a_S^{\rm out}(t)=(\gamma_S)^{1/2}a(t)-a_S^{\rm in}(t)\ . \tag{8}$$

The voltage $u_S^{\rm out}(t)$ of the outward traveling wave[6] across the signal transmission line may be expressed in terms of this output field according to

$$u_S^{\rm out}(t)=u_S^{{\rm out}(+)}(t)+u_S^{{\rm out}(-)}(t) \tag{9}$$

with

$$u_S^{{\rm out}(+)}(t)=-i\left[\frac{\hbar\Omega R_S}{2}\right]^{1/2}a_S^{\rm out}(t)e^{-i\Omega t}\ . \tag{10}$$

and

$$u_S^{{\rm out}(-)}(t)=u_S^{{\rm out}(+)}(t)^\dagger\ . \tag{11}$$

Thus Eqs. (8)–(11) allow us to calculate explicitly the properties of the outward traveling electromagnetic wave in terms of the statistics of the intracavity field $a(t)$ and $a_S^{\rm in}(t)$.

If we assume that the inward traveling modes of the transmission lines are in thermal equilibrium at temperatures T_R and T_S, respectively, we obtain for the expectation values of the input field correlations, for example,

$$\langle a_S^{\rm in}(t)a_S^{\rm in}(t)^\dagger\rangle=\int_{-\infty}^{+\infty}[n_S(\Omega+\omega)+1]e^{-i\omega(t-t')}d\omega \tag{12}$$

where $n_S(\omega)$ is the number of thermally excited photons in the mode with frequency ω and is given by

$$n_S(\omega)=\frac{1}{e^{\hbar\omega/kT_S}-1}\ . \tag{13}$$

If the number of excited photons does not vary much with frequency in the vicinity of the cavity mode frequency Ω, we can approximate the integral above by

$$\langle a_S^{\rm in}(t)a_S^{\rm in}(t')^\dagger\rangle=[n_S(\Omega)+1]\delta(t-t') \tag{14}$$

and analogously

$$\langle a_S^{\rm in}(t)^\dagger a_S^{\rm in}(t')\rangle=n_S(\Omega)\delta(t-t')\ . \tag{15}$$

Thus the input field can be approximated by quantum white noise.[11] Analogous expressions are valid for the input-field operator $a_R^{\rm in}(t)$. With this approximation the quantum Langevin equation (1) is explicitly of the type discussed by Gardiner and Collett[11] and they have shown that this quantum Langevin equation is equivalent to the following master equation for the density operator of the cavity mode:

$$\frac{d\rho}{dt}=-\frac{i}{\hbar}[\bar{H}_{\rm sys},\rho]+\left[\frac{\gamma_R}{2}(n_R+1)+\frac{\gamma_S}{2}(n_S+1)\right] \times([a,\rho a^\dagger]+[a\rho,a^\dagger]) +\left[\frac{\gamma_R}{2}n_R+\frac{\gamma_S}{2}n_S\right]([a^\dagger,\rho a]+[a^\dagger\rho,a])\ . \tag{16}$$

To obtain a degenerate dc-pumped parametric amplifier, we have to adjust the dc voltage V_0 according to Eq. (3),

so that the pump frequency ω_0 is just two times the signal frequency Ω. Then we obtain, for the averaged Hamiltonian in the rotating-wave approximation according to Eq. (2) by the Baker-Hausdorff theorem, a series expansion of the cosine, and doing the time average over one period of oscillation

$$\bar{H}_{\rm sys}=E_J-\frac{E_J}{2}e^{-s\kappa^2/2}\times\sum_{n=0}^{+\infty}\frac{(i\kappa)^{2n+2}}{n!(n+2)!}\{e^{i\varphi_0}[(a^\dagger)^n a^{n+2}]_s+e^{-i\varphi_0}[a^n(a^\dagger)^{n+2}]_s\} \tag{17}$$

where $s=\pm1$ denotes normal or antinormal ordering, respectively. For $s=0$ we obtain the symmetrically ordered Hamiltonian of the system with[12]

$$[(a^\dagger)^n a^m]_0=\frac{\partial^{n+m}}{\partial\beta^n\partial(-\beta^*)^m}e^{\beta a^\dagger-\beta^* a}\bigg|_{\beta=\beta^*=0}. \tag{18}$$

From Eq. (17) we can see that the ordering of the operators results in the factor $e^{-s\kappa^2/2}$ in front of the Hamiltonian. Therefore if the coupling constant κ becomes small the operator ordering does not matter much; that means for $\kappa\ll1$ the reversible part of the system dynamic approaches the classical dynamic, as we will show later on. If we had treated the DCPJPA classically we would have obtained, for the classical Hamiltonian of the system which is the symmetrically ordered Hamiltonian above, $s=0$, where the operators a and $a^\dagger$ are replaced by the classical amplitudes α and α^*. By doing this the sum can be added up and we obtain for the Hamiltonian of the classical system in the rotating-wave approximation

$$\bar{H}_{\rm cl}=E_J\left[1-\left[\frac{\alpha^2e^{i\varphi_0}+\alpha^{*2}e^{-i\varphi_0}}{2|\alpha|^2}\right]\right]J_2(2\kappa|\alpha|), \tag{19}$$

where J_n denotes the Bessel function of first kind and nth order. For a further investigation of the dynamics of the cavity mode, it is advantageous to represent the density operator by a quasiprobability distribution.[13] Here we will make use of the Wigner distribution, which allows direct computation of symmetrically ordered expectation values. The Wigner distribution $W(\alpha)$ of an operator ρ is defined by[14]

$$W(\alpha)=\mathrm{Tr}[\rho T(\alpha)], \tag{20}$$

where the operator $T(\alpha)$ is just the Fourier transform of the displacement operator

$$T(\alpha)=\int\frac{d^2\xi}{\pi}e^{\alpha\xi^*-\alpha^*\xi}e^{\xi a^\dagger-\xi^* a}. \tag{21}$$

As is shown in Appendix A, application of the definition (20) onto Eq. (16) results in the following evolution equation for the Wigner distribution of the density operator:

$$\frac{\partial W(\alpha,t)}{\partial t}=\left[\frac{\gamma}{2}\left[\frac{\partial}{\partial\alpha}\alpha+\frac{\partial}{\partial\alpha^*}\alpha^*\right]+\frac{\bar{\gamma}}{2}\frac{\partial^2}{\partial\alpha\,\partial\alpha^*}\right]W(\alpha,t)+\left[\frac{-iE_J\kappa}{2\hbar}e^{i\varphi_0}\sum_{n=0}^{\infty}\left[\frac{\kappa}{2}\right]^{2n}\sum_{m=0}^{2n+1}\frac{1}{m!(2n+1-m)!}\frac{\partial^m}{\partial\alpha^m}\frac{\partial^{2n+1-m}}{\partial(\alpha^*)^{2n+1-m}}\times\left[\frac{\alpha}{|\alpha|}\right]^{2m-2n+1}J_{2m-2n+1}(2\kappa|\alpha|)+\text{c.c.}\right]W(\alpha,t) \tag{22}$$

with

$$\bar{\gamma}=\gamma_R(2n_R+1)+\gamma_S(2n_S+1). \tag{23}$$

The first term in this equation results from the irreversible part of the master equation (16) which leads to damping of the cavity mode and fluctuations. The second term describes the reversible dynamic of the Josephson junction. Note that in the sum over n the nth term is a derivative of $(2n+1)$th order in α and α^* and every summand is reduced by a factor of $(\kappa/2)^{2n}$. It is well known[13] that the odd derivatives higher than one originate from the quantum properties of the process, that means from the noncommuting behavior of the annihilation and creation operators a and $a^\dagger$ in comparison to the classical amplitudes α and α^*, whereas the terms corresponding to the first derivatives can be interpreted as the drift term of a Fokker-Planck equation for a classical stochastic process, where the reversible part of the equation of motion originates from the classical Hamiltonian $H_{\rm cl}$ given in Eq. (19). As was already discussed in Ref. 6 the ratio $\kappa/2\pi$ is the average number of magnetic flux quanta stored in the inductance L if the resonator field is in the vacuum state $|0\rangle$. Therefore if the coupling constant κ is of the order of 2π, already the vacuum fluctuations of the cavity mode lead to magnetic flux fluctuations at the Josephson junction of the order of one flux quantum Φ_0. This of course means that the quantum-mechanical fluctuations associated with one photon drive the system into the strong nonlinear regime provided by the oscillation of the Josephson current if the magnetic flux in the inductance L changes by one flux quantum. Equation (22) clearly states that in this parameter regime one cannot neglect the higher derivatives originating from the quantum properties of the device. As will be seen in the forthcoming sections one can only achieve a considerable amount of squeezing in the outward traveling field if the

dominant loss mechanism of the device is the coupling to the signal transmission line. Therefore we can express the loaded quality factor Q_L by the capacitive part ΩC of the susceptance of the resonator at resonance and the load resistance R_S by

$$Q_L=\Omega C R_S \ . \tag{24}$$

Thus the coupling constant κ can be expressed by these basic device parameters according to Eq. (4) as

$$\kappa=\left[\frac{R_S}{R_\kappa Q_L}\right]^{1/2} \tag{25}$$

with $R_\kappa=\hbar/2e_0^2=2.054$ kΩ a given constant. Since R_S must be much smaller than the shunt resistance R of the Josephson junction which is maximum of the order of 1 kΩ, R_S has to be much smaller than R_κ. The loaded quality factor Q_L of the resonator must be much smaller than the unloaded, so that the resonator losses can be neglected. With superconducting resonators one can easily achieve quality factors as large as 10^5-10^6 therefore the loaded quality factor can be made as large as 10^3. With these data the coupling constant κ is about 10^{-3} in an experimental setup. Anyway, to achieve squeezing and to be in the range where the rotating-wave approximation is valid, that is, $Q_L \gg 1$, the coupling constant according to Eq. (25) always fulfills $\kappa \ll 1$. Therefore we can approximate the evolution equation for the Wigner distribution Eq. (22) by neglecting the derivatives of order greater than or equal to 3 because these terms are at least multiplied by an additional factor of $(\kappa/2)^2$ in comparison to the first-order term. Doing this we obtain the following approximated master equation for the Wigner distribution:

$$\frac{\partial W(\alpha,t)}{\partial t}=\left[\frac{\gamma}{2}\left[\frac{\partial}{\partial\alpha}\alpha+\frac{\partial}{\partial\alpha^*}\alpha^*\right]+\frac{\overline{\gamma}}{2}\frac{\partial^2}{\partial\alpha\,\partial\alpha^*}\right]W(\alpha,t)$$
$$+\left\{\frac{-iE_J\kappa}{2\hbar}e^{i\varphi_0}\left[\frac{\partial}{\partial\alpha}\left[\frac{\alpha}{|\alpha|}\right]^3 J_3(2\kappa|\alpha|)+\frac{\partial}{\partial\alpha^*}\frac{\alpha}{|\alpha|}J_1(2\kappa|\alpha|)\right]+\text{c.c.}\right\}W(\alpha,t)\ . \tag{26}$$

This is a Fokker-Planck equation corresponding to the Langevin equations

$$\dot\alpha=-\frac{\gamma}{2}\alpha-\frac{i}{\hbar}\frac{\partial H_{\rm cl}}{\partial\alpha^*}+(\gamma_S)^{1/2}\xi_S(t)+(\gamma_R)^{1/2}\xi_R(t)\ , \tag{27}$$

$$\dot\alpha^*=-\frac{\gamma}{2}\alpha^*+\frac{i}{\hbar}\frac{\partial H_{\rm cl}}{\partial\alpha}+(\gamma_S)^{1/2}\xi_S^*(t)+(\gamma_R)^{1/2}\xi_R^*(t) \tag{28}$$

where the variables ξ_S and ξ_R are independent complex Gaussian noise sources with

$$\langle\xi_i(t)\xi_i^*(t')\rangle=[n_i(\Omega)+\tfrac{1}{2}]\delta(t-t')\ , \tag{29}$$

$$\langle\xi_i(t)\xi_i(t')\rangle=0 \tag{30}$$

for $i=R,S$. To obtain the drift terms from $H_{\rm cl}$ according to Eq. (19) one has to use the recurrence relations for the Bessel functions

$$\frac{d}{dx}J_n(x)=\tfrac{1}{2}(J_{n-1}-J_{n+1})\ , \tag{31}$$

$$J_n(x)=\frac{x}{2n}(J_{n-1}+J_{n+1})\ . \tag{32}$$

Thus in the small coupling limit $\kappa \ll 1$ the dynamics of this degenerate Josephson amplifier can be treated in a classical manner, since the master equation for the density operator in the Wigner distribution representation is equivalent to a Fokker-Planck equation of a classical stochastic process. The only quantum-mechanical feature of the process surviving the approximations is the $\frac{1}{2}$ in Eq. (29) which represents the vacuum fluctuations of the transmission line fields coupled to the system. If the temperatures of these transmission lines tend to zero the thermally excited photons $n_{R,S}$ approach zero. But the vacuum fluctuations which are entirely of quantum-mechanical origin couple to the system again and prevent the Wigner distribution from becoming singular in the course of time, which is forbidden since it is the symmetrically ordered representation of the density operator of a quantum-mechanical system.[12,13] If we had no vacuum fluctuations in the zero-temperature limit the fluctuations would vanish. But without fluctuations the Wigner distribution would collapse to a Dirac δ distribution at the stable stationary points of the deterministic dynamic. This forbidden behavior for the quantum-mechanical Wigner distribution is prevented by the vacuum fluctuations.

III. STATIONARY POINTS AND STABILITY

To study the behavior of the solutions of the Fokker-Planck equation derived above we seek the stationary points of the deterministic part of the Langevin equations (27). Therefore we introduce the rescaled amplitude $\beta=2\kappa\alpha$ which obeys the Langevin equation

$$\dot\beta=-\frac{\gamma}{2}\beta-i\frac{E_J\kappa^2}{\hbar}\left[\frac{\beta^*}{|\beta|}e^{-i\varphi_0}J_1(|\beta|)-\left[\frac{\beta}{|\beta|}\right]^3 e^{i\varphi_0}J_3(|\beta|)\right]$$
$$+2\kappa[(\gamma_S)^{1/2}\xi_S(t)+(\gamma_R)^{1/2}\xi_R(t)]\ . \tag{33}$$

Thus for $\kappa \ll 1$, as is the case, the classical trajectories $\beta(t)$ only make small fluctuations around the stable stationary points β_0.

A. Stationary points

The stationary points of the deterministic part of the above Langevin equation are obtained by setting $\dot{\beta}_0=0$. And with

$$\beta_0=re^{i\varphi} \tag{34}$$

we obtain from Eq. (33)

$$r=-2ip[e^{-i(2\varphi+\varphi_0)}J_1(r)-e^{i(2\varphi+\varphi_0)}J_3(r)] \tag{35}$$

where we have introduced the pump parameter

$$p=\frac{E_J\kappa^2}{\hbar\gamma} . \tag{36}$$

Setting the real and imaginary parts of Eq. (35) equal to zero yields, with the recurrence relations of the Bessel functions (31) and (32),

$$r^2=-8pJ_2(r)\sin(2\varphi+\varphi_0) \tag{37}$$

and

$$\cos(2\varphi+\varphi_0)J_2'(r)=0 . \tag{38}$$

This equation implies a differentiation between the following two cases.

1. Case 1

We set

$$\cos(2\varphi+\varphi_0)=0 , \tag{39a}$$

$$\varphi_n^{(1)}=-\frac{\varphi_0}{2}+\frac{(2n-1)\pi}{4} \quad \text{for } 0\le n\le 3 \tag{39b}$$

and from Eq. (37) we obtain

$$(-1)^n(r^{(1)})^2=8pJ_2(r^{(1)}) . \tag{40}$$

The existence and dependence of the different roots of this equation on the pump parameter p can be seen from Fig. 2. The graphical solution of Eq. (40) is shown there. That is the cross point of the positive or negative parabola with $8p$ times the Bessel function of second order; in Fig. 2 $p=1$. A series expansion of this Bessel function given by

$$J_2(x)=\tfrac{1}{8}x^2-\tfrac{1}{96}x^4+O(x^6) \tag{41}$$

shows by comparison with Eq. (40) that for $p<1$ the only solution is $r_0^{(1)}=0$. For the critical value $p=p_{c1}^{(1)}=1$ a bifurcation takes place and two branches of stationary states in the directions $\varphi_n^{(1)}$ according to Eq. (39b) with $n=0,2$ go away from the origin since the Bessel function crosses the positive branch of the parabola. If we further increase the pump parameter p a second bifurcation point $p=p_{c2}^{(1)}$ is reached where the Bessel function touches the negative branch of the parabola, see Fig. 3. At this bifurcation point four new branches of stationary points are

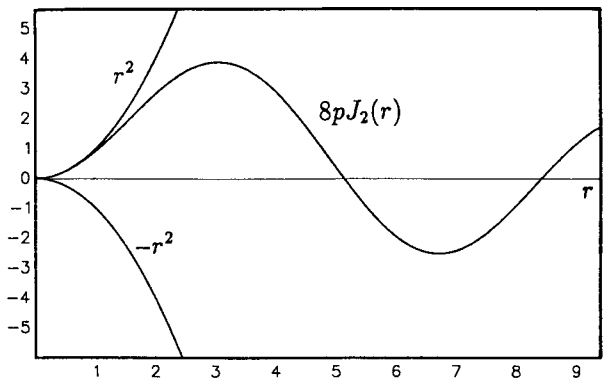

FIG. 2. Graphical solution of Eq. (40) for $p=1$.

created, since for every new value of the amplitude there are two allowed phase angles given by Eq. (40) for $n=1,3$. If we further increase the pump parameter the Bessel function alternatively cuts the positive and negative parabola. The critical values of the pump parameter where these bifurcations occur and the corresponding critical amplitudes $r_{c_m}^{(1)}$ can be determined from two conditions: First they must obey Eq. (40) and second the derivative of this equation with respect to the amplitude.

$$(-1)^n r_{c_m}^{(1)}=4pJ_2'(r_{c_m}^{(1)}) \tag{42}$$

may also be fulfilled since at the bifurcation point the Bessel function just touches one of the parabola's branches as shown, for example, in Fig. 3. From these two equations it follows that we obtain the critical amplitudes by solving the equation

$$\tfrac{1}{2}r_{c_m}^{(1)}J_2'(r_{c_m}^{(1)})=J_2(r_{c_m}^{(1)}) \tag{43}$$

and the critical pump parameters can be determined subsequently by

$$p_{c_m}^{(1)}=\left|\frac{(r_{c_m}^{(1)})^2}{8J_2(r_{c_m}^{(1)})}\right| . \tag{44}$$

These critical amplitudes and the corresponding critical pump parameters are listed in Table I.

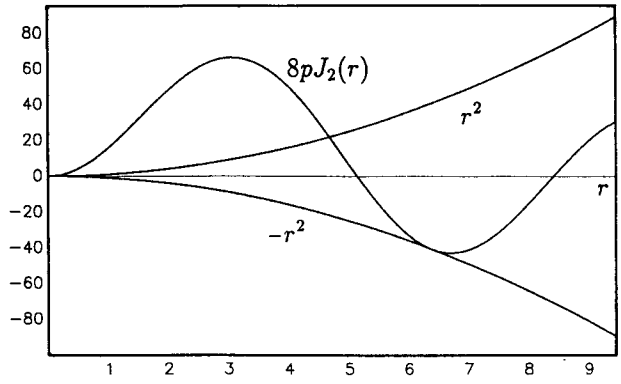

FIG. 3. Graphical solution of Eq. (40) for $p=p_{c_2}^{(1)}$.

TABLE I. Critical values of the pump parameter and accompanying amplitudes for case-1 and -2 stationary solutions.

	Case 1		Case 2	
n	$p_{c_n}^{(1)}$	$r_{c_n}^{(1)}$	$p_{c_n}^{(2)}$	$r_{c_n}^{(2)}$
1	1.00	0.00	2.40	3.05
2	17.06	6.38	17.93	6.71
3	47.75	9.76	48.77	9.97
4	97.01	13.02	98.16	13.17
5	167.49	16.22	169.02	16.35

2. Case 2

In the second case the roots of the derivative of the Bessel function of first kind and second order determine the amplitudes of the stationary states according to Eq. (38):

$$J_2'(r_m^{(2)})=0 . \tag{45}$$

The first few roots of this equation are also listed in Table I and the corresponding phase angles can be obtained according to Eq. (37) by

$$\varphi_{n,m}^{(2)}=-\frac{\varphi_0}{2}+\frac{n\pi}{2}+(-1)^n\frac{1}{2}\arcsin\left[\frac{-(r_m^{(2)})^2}{8pJ_2(r_m^{(2)})}\right] \quad \text{for } 0\le n\le 3 . \tag{46}$$

Note that this equation has only a solution for those r_m for which the absolute value of the argument of the arcsin function is less than 1. Therefore there exists a lower limit for the pump parameter

$$p=p_{c_m}^{(2)}=\left|\frac{(r_m^{(2)})^2}{8J_2(r_m^{(2)})}\right| . \tag{47}$$

Below this value Eq. (46) has no solution. These critical pump parameters for the corresponding amplitudes are also shown in Table I.

B. Stability of the stationary points

To show the stability properties of the various stationary points, we linearize the deterministic part of the Langevin equation (33) and the corresponding complex conjugate equation at the stationary points. Thus we obtain for the deviation from the stationary value $\Delta\beta=\beta-\beta_0$ and its complex conjugate the set of linear differential equation

$$\dot{\Delta\beta}=\left[-\frac{\gamma}{2}+i\Delta\right]\Delta\beta+g\Delta\beta^* , \tag{48}$$

$$\dot{\Delta\beta}^*=\left[-\frac{\gamma}{2}-i\Delta\right]\Delta\beta^*+g^*\Delta\beta , \tag{49}$$

with

$$\Delta=\gamma pJ_2(r)\cos(2\varphi+\varphi_0) , \tag{50}$$

$$g=-i\frac{\gamma p}{2}e^{-i\varphi_0}[J_0(r)+J_4(r)e^{i2(2\varphi+\varphi_0)}] , \tag{51}$$

where g is the conversion coefficient of the parametric process. The characteristic exponents of these linear differential equations are given by

$$\lambda_{1/2}=-\frac{\gamma}{2}\pm(|g|^2-\Delta^2)^{1/2} . \tag{52}$$

The stationary states are stable if the real parts of both characteristic exponents are positive. Thus the stationary states are stable if the condition

$$\left[\frac{\gamma}{2}\right]^2>|g|^2-\Delta^2 \tag{53}$$

is fulfilled. With relations (39) and (40) for the stationary states of case 1 this stability condition can be transformed to

$$1>\left|1-\frac{J_2'(r^{(1)})}{(-1)^n r^{(1)}}8p\right| , \tag{54}$$

as is shown in Appendix B, Sec. 1. The stationary states in case 2, obeying the relations (45) and (46), are always stable, as is shown in Appendix B, Sec. 2.

C. Bifurcation diagram

With the results of the preceding sections the bifurcation and stability diagram of the DCPJPA in the complex β plane as it is shown in Fig. 4 can be constructed. In the following discussion we will set the phase shift $\varphi_0=0$ because it results only in a trivial rotation of the β plane by an angle $\varphi_0/2$. For $0<p<p_{c_1}^{(1)}=1$ the origin is the only stable stationary point. For $p>p_{c_1}^{(1)}$ the origin becomes unstable and two branches of stable case-1 solutions start

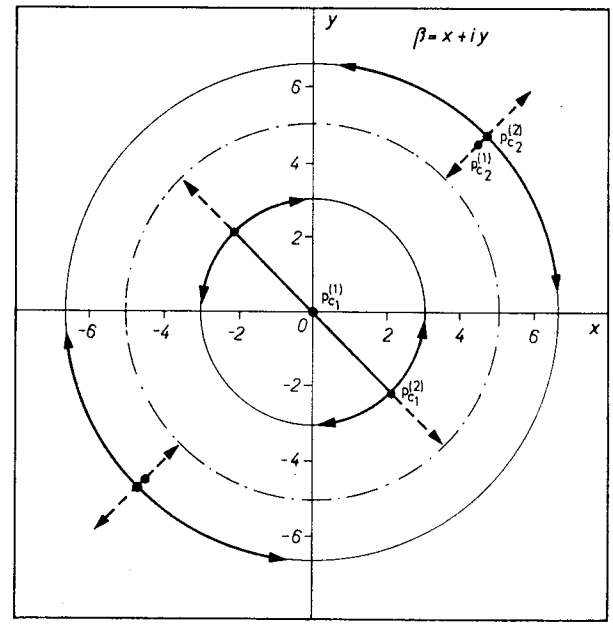

FIG. 4. Bifurcation diagram for the DCPJPA: – – –, unstable stationary states; ——, stable stationary states; –·–·–·, $J_2(r)=0$.

from the origin along the rays with $\varphi_{0,2}^{(1)}$ according to Eq. (39). When the pump parameter p reaches the first critical value $p_{c_1}^{(2)}$ of the case-2 solutions, see Table I, the amplitude reaches a zero of the derivative of the Bessel function and two new stable branches of case-2 stationary states are created at that bifurcation point, see Fig. 4. The old branches of case-1 stationary states change stability properties at that point according to condition (54) and become unstable. If the pump parameter is further increased the amplitude $r_1^{(1)}$ approaches the zero of the second-order Bessel function, as can be seen from Fig. 3. The amplitudes of the newly created stable stationary points are left constant whereas the phase angles approach the coordinate axes with increasing pump parameter. When the pump parameter reaches the critical point $p=p_{c_2}^{(1)}$, see Fig. 3 and Table I, two new branches of stationary case-1 solutions are created, but the phase angles according to Eq. (39) are now determined by $n=1,3$. Note that the inward moving branches are unstable and the outward moving branches are stable according to condition (54). If the pump parameter p is further increased one reaches the next critical value $p_{c_2}^{(2)}$ for case-2 stationary states and the bifurcation behavior as discussed at the critical value $p_{c_1}^{(2)}$ will occur again only the phase angles have changed according to Eq. (46). Increasing the pump parameter p further on one alternatively reaches a case-1 and case-2 critical point, see Table I, with the bifurcation behavior discussed above.

IV. SQUEEZING OF THE RADIATION FIELD

If the device operates far away from bifurcation points, we can linearize the Langevin equation (33) in the vicinity of a stable stationary point. Therefore we obtain linearized Langevin equations for the deviation of the intracavity field from the stationary value $\alpha_0=\beta_0/2\kappa$:

$$\underline{\Delta\alpha}=\underline{A}\,\underline{\Delta\alpha}+(\gamma_S)^{1/2}\underline{\xi}_S+(\gamma_R)^{1/2}\underline{\xi}_R \tag{55}$$

where

$$\underline{\Delta\alpha}^T=(\Delta\alpha,\Delta\alpha^*),\quad \underline{\xi}_i^T=(\xi_i(t),\xi_i^*(t))\quad \text{for } i=R,S \tag{56}$$

and

$$\underline{A}=\begin{bmatrix}-\gamma/2+i\Delta & g\\ g^* & -\gamma/2-i\Delta\end{bmatrix}. \tag{57}$$

Since these Langevin equations were derived from the Wigner distribution representation, averages computed by these Langevin equations have to be understood as the averages over the corresponding symmetrically ordered operator expressions. To be able to calculate statistical properties of the output field one has to relate the statistical behavior of the output field to that of the intracavity field as it was done by the operator expression given by Eq. (8). Reynaud and Heidmann[9] have shown that the quantum-mechanically correct squeezing spectrum of the output field of the degenerate parametric amplifier can be computed from the Langevin equation above when the input-output relation Eq. (8) is also transformed into a c-number equation, where the input field is again expressed as the white Gaussian noise source $\xi_S(t)$, that is,

$$\underline{\Delta\alpha}^{\text{out}}=(\gamma_S)^{1/2}\underline{\Delta\alpha}-\underline{\xi}_S(t)\ . \tag{58}$$

One can show by a rigorous quantum-mechanical calculation (to be published elsewhere), that whenever the time evolution of the Wigner distribution is equivalent to a Fokker-Planck equation, one can compute the quantum-mechanically correct squeezing spectrum from the corresponding classical Langevin equations and the classical input-output relation Eq. (58).

A. Squeezing of the intracavity field

The squeezing of the intracavity field is defined via the variances of the quadrature components

$$\Delta A_\theta=\tfrac{1}{2}(\Delta a e^{i\theta}+\Delta a^\dagger e^{-i\theta})\ . \tag{59}$$

Since the square of the variance of this component is a symmetrically ordered operator expression we obtain

$$\langle(\Delta A_\theta)^2\rangle=\tfrac{1}{4}\langle(\Delta a e^{i\theta}+\Delta\alpha^* e^{-i\theta})^2\rangle\ . \tag{60}$$

The value of this expression can be easily calculated from the set of linear Langevin equations (55) above and we obtain

$$\langle(\Delta A_\theta)^2\rangle=\frac{\bar\gamma}{16\gamma}\left[\frac{\gamma^2+4\Delta^2+4|g|[(\gamma/2)^2+\Delta^2]^{1/2}\cos(\chi+\chi_0+2\theta)}{(\gamma/2)^2+\Delta^2-|g|^2}\right], \tag{61}$$

where

$$\chi=\arg[g]=-\frac{\pi}{2}-\varphi_0+\arg[J_0(r)+J_4(r)e^{i2(2\varphi+\varphi_0)}] \tag{62}$$

$$\chi_0=\arctan\left[\frac{2\Delta}{\gamma}\right], \tag{63}$$

and $\bar\gamma$ is given by Eq. (23). Thus the quadrature component with θ equal to

$$\theta_{\min}=\frac{\pi}{2}-\tfrac{1}{2}(\chi+\chi_0) \tag{64}$$

has the minimum fluctuations

$$\langle(\Delta A_{\theta_{\min}})^2\rangle=\frac{1}{4}\left[1+2\frac{\gamma_R}{\gamma}n_R+2\frac{\gamma_S}{\gamma}n_S\right]\times\frac{[(\gamma/2)^2+\Delta^2]^{1/2}}{[(\gamma/2)^2+\Delta^2]^{1/2}+|g|}\ . \tag{65}$$

From this expression one can see that whenever a bifurcation point is reached, that means one of the eigenvalues $\lambda_{1/2}$ according to Eq. (52) is zero, the fluctuations in this quadrature component reach the absolute minimum value

$$\langle(\Delta A_{\theta_{\min}})^2\rangle_{\min}=\frac{1}{8}\left[1+2\frac{\gamma_R}{\gamma}n_R+2\frac{\gamma_S}{\gamma}n_S\right]. \quad (66)$$

Thus if the temperatures of the transmission lines approach zero we obtain just half of the fluctuations with respect to the vacuum state for one of the intracavity field quadrature components. The fluctuations in the quadrature component with $\theta=\theta_{\max}=\theta_{\min}+\pi/2$ go to infinity at these bifurcation points. For case-1 stationary points we obtain from Eqs. (39), (62)–(64)

$$\theta_{\min}^{(1)}=\frac{3\pi}{4}+\frac{\varphi_0}{2}-u(J_4(r^{(1)})-J_0(r^{(1)}))\frac{\pi}{2} \quad (67)$$

with the Heaviside function

$$u(x)=\begin{cases}0, & x\le 0\\ 1, & x>0\end{cases}. \quad (68)$$

The additional phase $\pi/2$ in Eq. (67) arises when the argument of the last term in Eq. (62) is in the second or third quadrant of the complex plane. For case-2 stationary points we get, from Eqs. (45), (46), (31), and (32),

$$J_0(r_m^{(2)})=J_2(r_m^{(2)})\left[\frac{4}{(r_m^{(2)})^2}-1\right], \quad (69)$$

$$J_4(r_m^{(2)})=J_2(r_m^{(2)})\left[\frac{12}{(r_m^{(2)})^2}-1\right], \quad (70)$$

and therefore with Eqs. (62)–(64)

$$\theta_{\min}^{(2)}=\frac{3\pi}{4}+\frac{\varphi_0}{2}+\frac{(-1)^n}{2}\left[\arctan\left[\frac{(r_m^{(2)})^2}{4\tan(\varphi_{0,m}^{(2)})}\right]-\arctan\left[\frac{y}{x}\right]-u(-x)\pi\right] \quad (71)$$

with

$$x=4-(r_m^{(2)})^2+[12-(r_m^{(2)})^2]\cos(\varphi_{0,m}^{(2)}), \quad (72)$$

$$y=[12-(r_m^{(2)})^2]\cos(\varphi_{0,m}^{(2)}). \quad (73)$$

With this information we can sketch the stationary solutions of the linearized Fokker-Planck equation, which is a Gaussian distribution, for the different parameter regimes. As before the phase shift φ_0 will be set to zero. As usual[15] the Gaussian distribution will be represented by its error ellipse. Note that the direction of minimum fluctuations has the angle $-\theta_{\min}$ in the complex α plane. Thus for $p<p_{c_1}^{(1)}$ a squeezed vacuum state, as shown in Fig. 5(a), is obtained where the direction of minimum fluctuations is determined according to Eq. (67) to be $-\theta_{\min}^{(1)}=\pi/4$. When we approach the bifurcation point $p=p_{c_1}^{(1)}=1$ the squeezing becomes maximum as discussed above. If the pump parameter p is further increased, above this bifurcation point, we obtain two new stable case-1 stationary solutions, see Fig. 4, and therefore the stationary Wigner distribution becomes double peaked and looks like that shown in Fig. 5(b), which is a superposition of two phase squeezed states. But above threshold the squeezing will decrease because the absolute value of the conversion coefficient g decreases according to Eq. (51) until the pump parameter reaches the value $p=p_1^{(0)}$ with corresponding amplitude $r=r_1^{(0)}$ which is determined by the vanishing of the conversion coefficient g. Thus from Eqs. (39) and (51) $r_1^{(0)}$ is determined by the first root of the equation

$$J_0(r_1^{(0)})-J_4(r_1^{(0)})=0 \quad (74)$$

which is $r_1^{(0)}\simeq 2.3$ and from Eq. (44) we get for the corresponding pump parameter $p_1^{(0)}\simeq 1.6$. At this parameter value no squeezing occurs at all and we have a superposition of two coherent states, see Fig. 5(c). Above this parameter value the Gaussian distribution will become squeezed again, but the angle where minimum fluctuations occur has changed to $\theta_{\min}=\pi/4$ due to the change of sign of the expression (74) in Eq. (67), leading to a superposition of two amplitude squeezed states, see Fig. 5(d). When we reach the second bifurcation point $p_{c_1}^{(2)}$ the squeezing in this direction becomes maximum. If the coupling coefficient κ is small enough the two Gaussian

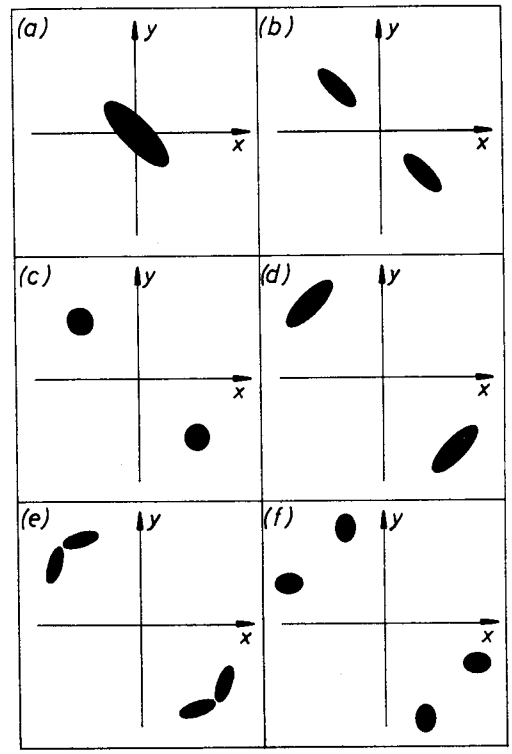

FIG. 5. Sketch of the stationary solution of the linearized Fokker-Planck equation for different values of the pump parameter: (a) $0<p<p_{c_1}^{(1)}$, (b) $p_{c_1}^{(1)}<p<p_{c_1}^{(0)}$, (c) $p=p_{c_1}^{(0)}$, (d) $p_{c_1}^{(0)}<p<p_{c_1}^{(2)}$, (e) $p=2.55$, (f) $p=3.42$.

distributions are far away from each other, so that there will be almost no transitions between these two Gaussian distributions and the field mode in the DCPJPA at this second threshold is then in one definite amplitude squeezed state.

If we further increase the pump parameter into the region $p_{c_1}^{(2)} < p < p_{c_2}^{(1)}$ the old case-1 stable stationary states vanish and four new stable case-2 stationary states are created according to Fig. 4. Figures 5(e) and 5(f) show the Wigner distributions for two values of the pump parameter p in this regime. The squeezing of these states continuously degrades for increasing pump parameters. For $p > p_{c_2}^{(1)}$ additional Gaussian distributions must be added at the newly created stable stationary solutions, see Fig. 4. But we will not discuss their behavior with respect to squeezing further on, since the observed behavior is an average over all the Gaussian distributions at the stable stationary solutions, which smears out the squeezing behavior of the single Gaussian distribution.

B. Spectral squeezing of the output field

The field experimentally observable is the outward traveling field on the signal transmission line. The squeezing behavior of this field is usually characterized by the squeezing spectra $S_\theta^{\text{out}}(\omega)$ (Refs. 6 and 16) and is defined as the Fourier transform of the autocorrelation function

$$c_\theta^{\text{out}}(\tau) = \langle \Delta A_\theta^{\text{out}}(\tau) \Delta A_\theta^{\text{out}}(0) \rangle \tag{75}$$

of the quadrature component of the output field

$$\Delta A_\theta^{\text{out}} = \tfrac{1}{2}(\Delta a_S^{\text{out}} e^{i\theta} + \Delta a_S^{\text{out}+} e^{-i\theta}) \tag{76}$$

by

$$S_\theta^{\text{out}}(\omega) = \int_{-\infty}^{\infty} c_\theta^{\text{out}}(\tau) e^{i\omega\tau} d\tau \, . \tag{77}$$

The semiclassical input-output formalism of Reynaud and Heidmann as discussed above states that the correlation function (75) is equivalent to

$$c_\theta^{\text{out}}(\tau) = \langle \Delta\alpha_\theta^{\text{out}}(\tau) \Delta\alpha_\theta^{\text{out}}(0) \rangle \tag{78}$$

where $\Delta\alpha$ obeys the Langevin equations (55) and the input-output relations (58). Since we have a set of linear Langevin equations the squeezing spectrum can be easily computed in the frequency domain[9] and we obtain for $T_R = T_S$ and therefore $n_R = n_S = n$

$$S_\theta^{\text{out}}(\omega) = \frac{n+\frac{1}{2}}{2}\left[1 + \frac{2\gamma_S|g|}{|\det(\omega)|^2}\left[\gamma|g| + \left\{\left[\left[\frac{\gamma}{2}\right]^2 - \Delta^2 + |g|^2 + \omega^2\right]^2 + \Delta^2\gamma^2\right\}^{1/2} \cos(2\theta + \chi + \chi_0')\right]\right], \tag{79}$$

where

$$\det(\omega) = \left[\frac{\gamma}{2} - i\omega\right]^2 + \Delta^2 - |g|^2 \, , \tag{80}$$

$$\chi_0' = \arctan\left[\frac{\Delta\gamma}{(\gamma/2)^2 - \Delta^2 + \omega^2 + |g|^2}\right] . \tag{81}$$

As for the intracavity field the squeezing spectrum is minimum for a given frequency when we choose

$$\theta = \theta_{\min}^{\text{out}} = \frac{\pi}{2} - \tfrac{1}{2}(\chi + \chi_0') \, . \tag{82}$$

Note that for $\Delta \neq 0$ this angle depends via Eq. (81) on the frequency where one will observe minimum fluctuations. But as we have seen above the parameter values where the device is of experimental interest for the generation of squeezed states will be $p \leq p_{c_1}^{(2)}$. In this range there will only exist case-1 stationary solutions, where $\Delta = 0$ and therefore also $\chi_0' = 0$. Thus one can see from Eqs. (67) and (82) that in this regime the angle where minimum fluctuations can be obtained is the same for the intracavity and the output field. The squeezing spectrum of the output field takes on its absolute minimum value at the two bifurcation points $p_{c_1}^{(1)} = 1$ and $p_{c_1}^{(2)} = 2.4$ at frequency $\omega = 0$:

$$S_{\theta_{\min}}^{\text{out}}(0) = \frac{n+\frac{1}{2}}{2}\frac{\gamma_R}{\gamma} = \frac{n+\frac{1}{2}}{2}\frac{R_S}{R_S+R} = \frac{n+\frac{1}{2}}{2} r \tag{83}$$

where r denotes the noise reduction

$$r = \frac{R_S}{R_S + R} \tag{84}$$

below the thermal and vacuum noise level. Thus if r approaches zero, that means that the losses due to the junction resistance R are much smaller than those due to the coupling of the signal transmission line represented by R_S, this linear analysis predicts perfect squeezing of the output field around the center frequency of the cavity mode. Note that additional losses due to an imperfect cavity would have the same degrading effect on squeezing as the junction losses. Our result for the achievable squeezing for the DCPJPA agrees with the result for the external pumped JPA analyzed by Yurke[17] below the threshold for oscillation. Above threshold for oscillation and especially at $p = p_{c_1}^{(2)}$ the DCPJPA is an oscillator emitting a signal with mean amplitude $|\alpha_0| = (1/2\kappa) r_{c_1}^2$ and vanishing amplitude fluctuations for $r \to 0$.

V. OUTPUT POWER OF THE OSCILLATOR

The power radiated into the signal transmission line is given by

$$P^{\text{out}} = \frac{2}{R_S} \langle u_S^{\text{out}(-)} u_S^{\text{out}(+)} \rangle \, . \tag{85}$$

Assuming $T_R = T_S = 0$ so that the thermal noise vanishes,

we obtain with Eqs. (8)–(11)

$$P^{\text{out}}=\frac{\hbar\Omega}{R_S C}\langle a^\dagger(t)a(t)\rangle \ . \tag{86}$$

Thus the output power of the oscillator is given by the mean number of photons stored in the resonator multiplied by the energy of one photon and the damping rate due to the coupling of the resonator to the transmission line. Expressing the number operator by the symmetrically ordered expansion

$$a^\dagger a=\tfrac{1}{2}(a^\dagger a+aa^\dagger)-\tfrac{1}{2} \tag{87}$$

leads to the following result for the output in terms of averages built with the Wigner distribution:

$$P^{\text{out}}=\frac{\hbar\Omega}{R_S C}(\langle\alpha^*\alpha\rangle-\tfrac{1}{2}) \tag{88}$$

and therefore in the linear approach

$$P^{\text{out}}=\frac{\hbar\Omega}{R_S C}(|\alpha_0|^2+\langle\Delta\alpha^*\Delta\alpha\rangle-\tfrac{1}{2}) \ . \tag{89}$$

The first term is the output power due to the mean amplitude and the other terms represent the additional power due to the fluctuations of the field mode. If we neglect this fluctuation term the output power of the oscillator at the bifurcation point $p_{c_1}^{(2)}$, where the mean amplitude and the amplitude squeezing are maximum, is given by

$$P^{\text{out}}=\frac{\hbar\Omega(r_1^{(2)})^2}{R_S C|2\kappa|^2}=19.9\frac{f^2}{R_S}\text{pW}\frac{\Omega}{\text{GHz}^2} \tag{90}$$

where we have used Eq. (4). Note that the Ω in the last expression denotes the unit of resistance. According to Eqs. (4)–(6) and (36) the pump parameter p can be expressed by

$$p=\frac{r}{2}\frac{I_c R}{\Phi_0 f} \ . \tag{91}$$

The product $I_c R$ is a constant for a given Josephson junction. For a junction fabricated by usual low-temperature superconductors this product is about 1 mV. Since this voltage is proportional to the energy gap of the superconductor and therefore to the transition temperature it may be increased by the use of high-T_c superconductors. Therefore the requirement that the device works at the bifurcation point $p_{c_1}^{(2)}$ establishes via Eq. (91) a fixed relationship between the operation frequency and the noise reduction r:

$$f=100.7rI_c R \ \text{GHz/mV} \ . \tag{92}$$

Thus for a given superconductor the junction resistance R and the characteristic impedance R_S of the signal transmission line uniquely determine the frequency and the output power of the amplitude squeezed oscillator via Eqs. (92) and (90). To achieve a noise reduction of at least 0.1, the frequency is 10 GHz and the output power will be in the range of $2nW-2\ \mu$W for $1\Omega > R_S > 1\ \text{m}\Omega$.

VI. CONCLUSION

We have shown that the DCPJPA can be used to generate a squeezed vacuum state at the threshold for oscillation. Above this threshold a second bifurcation point exists, where the device generates amplitude squeezed radiation. Due to the relationship between squeezing and operation frequency, the frequency range where amplitude squeezed radiation can be achieved is below 100 GHz for usual low-temperature superconductors. This range can only be increased by the use of high-T_c superconductors for junction fabrication. Since the linearized analysis predicts maximum squeezing at the bifurcation points, where the linearization is not valid, one has to solve the complete Fokker-Planck equation (26) to obtain the maximum achievable squeezing and the stationary solution exactly, as will be done in a forthcoming paper.

APPENDIX A: DERIVATION OF THE MASTER EQUATION IN THE WIGNER DISTRIBUTION REPRESENTATION

To derive Eq. (22) we have to show some operator identities. For the operator $T(\alpha)$ according to Eq. (21) the following relations hold:

$$[(a^\dagger)^n a^m]_0 T(\alpha)=\sum_{k=0}^{n}\sum_{l=0}^{m}\begin{bmatrix}n\\k\end{bmatrix}\begin{bmatrix}m\\l\end{bmatrix}\left[\frac{1}{2}\frac{\partial}{\partial\alpha}\right]^k \times\left[-\frac{1}{2}\frac{\partial}{\partial\alpha^*}\right]^l(\alpha^*)^{n-k} \times\alpha^{n-l}T(\alpha) \ , \tag{A1}$$

$$T(\alpha)[(a^\dagger)^n a^m]_0=\sum_{k=0}^{n}\sum_{l=0}^{m}\begin{bmatrix}n\\k\end{bmatrix}\begin{bmatrix}m\\l\end{bmatrix}\left[-\frac{1}{2}\frac{\partial}{\partial\alpha}\right]^k \times\left[\frac{1}{2}\frac{\partial}{\partial\alpha^*}\right]^l(\alpha^*)^{n-k} \times\alpha^{n-l}T(\alpha) \ . \tag{A2}$$

The proof of Eq. (A1) can be easily done by the representation (18) of the symmetrically ordered product because

$$[(a^\dagger)^n a^m]_0 T(\alpha)=\frac{\partial^{n+m}}{\partial\beta^n\partial(-\beta^*)^m}\int\frac{d^2\xi}{\pi}\exp[(\alpha+\beta/2)\xi^*-(\alpha+\beta/2)^*\xi]\exp[(\xi+\beta)a^\dagger-(\xi+\beta)^*a]|_{\beta=\beta^*=0} \ , \tag{A3}$$

where we have used the Baker-Haussdorf theorem. Pulling the derivatives behind the first factor of the integrand results in

$$[(a^\dagger)^n a^m]_0 T(\alpha)=\int \frac{d^2\xi}{\pi}\exp[(\alpha+\beta/2)\xi^*-(\alpha+\beta/2)^*\xi]\left[\frac{\partial}{\partial\beta}+\frac{\xi^*}{2}\right]^n\left[\frac{\partial}{\partial(-\beta^*)}+\frac{\xi}{2}\right]^m$$
$$\times\exp[(\xi+\beta)a^\dagger-(\xi^*+\beta^*)a]|_{\beta=\beta^*=0}\,. \tag{A4}$$

Making use of the binomial formula, replacing the derivatives with respect to β by those with respect to ξ, and partial integration results in Eq. (A1). Equation (A2) can be derived analogously. Setting $\{n,m\}\in\{0,1\}$ into these equations yields for the irreversible part of the time evolution of the master equation (16)

$$\left.\frac{\partial W}{\partial t}\right|_{\rm irr}=\left[\frac{\gamma}{2}\left[\frac{\partial}{\partial\alpha}\alpha+\frac{\partial}{\partial\alpha^*}\alpha^*\right]+\frac{\bar\gamma}{2}\frac{\partial^2}{\partial\alpha\partial\alpha^*}\right]W(\alpha,t)\,. \tag{A5}$$

For the reversible part

$$\left.\frac{\partial W}{\partial t}\right|_{\rm rev}={\rm Tr}\left[-\frac{i}{\hbar}[\bar H_{\rm sys},\rho]T(\alpha)\right] \tag{A6}$$

we obtain with Eqs. (A1), (A2), and (17)

$$\left.\frac{\partial W}{\partial t}\right|_{\rm rev}=\left[\frac{-iE_J\kappa}{2\hbar}e^{i\varphi_0}\sum_{n=0}^{\infty}\sum_{k=0}^{n}\sum_{l=0}^{n+2}\frac{\kappa^{2n+1}(-1)^{n+2-l}}{2^{k+l}k!(n-k)!l!(n+2-l)!}[1-(-1)^{(k+l)}]\right.$$
$$\left.\times\left[\frac{\partial}{\partial\alpha}\right]^k\left[\frac{\partial}{\partial\alpha^*}\right]^l(\alpha^*)^{n-k}(\alpha)^{n+2-l}+{\rm c.c.}\right]W(\alpha,t)\,. \tag{A7}$$

Substituting $n-k=m$ and replacing the last factorial by Euler's gamma function so that it is also defined for negative arguments yields

$$\left.\frac{\partial W}{\partial t}\right|_{\rm rev}=\left[\frac{-iE_J\kappa}{2\hbar}e^{i\varphi_0}\sum_{k=0}^{\infty}\sum_{l=0}^{\infty}\frac{\kappa^{k+l-1}(-1)^{k-l}}{2^{k+l}k!l!}[1-(-1)^{(k+l)}]\left[\frac{\partial}{\partial\alpha}\right]^k\left[\frac{\partial}{\partial\alpha^*}\right]^l\right.$$
$$\left.\times\left[\frac{\alpha}{|\alpha|}\right]^{k-l+2}J_{2+k-l}(2\kappa|\alpha|)+{\rm c.c.}\right]W(\alpha,t)\,. \tag{A8}$$

Setting $k+l=s$ the terms in s cancel and we obtain for $s=2n+1$

$$\left.\frac{\partial W}{\partial t}\right|_{\rm rev}=\left[\frac{-iE_J\kappa}{2\hbar}e^{i\varphi_0}\sum_{n=0}^{\infty}\sum_{k=0}^{2n+1}\left[\frac{\kappa}{2}\right]^{2n}\frac{1}{k!(2n+1-k)!}\left[\frac{\partial}{\partial\alpha}\right]^k\left[\frac{\partial}{\partial\alpha^*}\right]^{2n+1-k}\right.$$
$$\left.\times\left[\frac{\alpha}{|\alpha|}\right]^{2k-2n+1}J_{2k-2n+1}(2\kappa|\alpha|)+{\rm c.c.}\right]W(\alpha,t)\,, \tag{A9}$$

the reversible part of Eq. (22).

APPENDIX B: STABILITY OF STATIONARY STATES

1. Case 1

For case-1 stationary states Eqs. (39) and (40) imply in Eqs. (50) and (51)

$$\Delta=0\quad\text{and}\quad|g|=\frac{\gamma p}{2}|J_0(r^{(1)})-J_4(r^{(1)})|\,. \tag{B1}$$

Using the recurrence relations for the Bessel functions Eqs. (31) and (32) one can show

$$x^2[J_0(x)-J_4(x)]=8[xJ_2'(x)-J_2(x)]\,. \tag{B2}$$

From that and Eq. (B1) the stability condition (53) is transformed to

$$1>\frac{8p}{(r^{(1)})^2}|r^{(1)}J_2'(r^{(1)})-J_2(r^{(1)})| \tag{B3}$$

and with Eq. (40) we obtain the desired result (54).

2. Case 2

For case-2 stationary states Eqs. (45), (46), (50), and (51) yield for the stability condition (53)

$$1>p^2(\{[J_0(r^{(2)})+J_4(r^{(2)})]^2-4[J_2(r^{(2)})]^2\}$$
$$\times\cos^2(2\varphi+\varphi_0)+[J_0(r^{(2)})-J_4(r^{(2)})]^2$$
$$\times\sin^2(2\varphi+\varphi_0))\,. \tag{B4}$$

Using Eq. (B2) to simplify the second term of this equa-

tion we obtain with Eqs. (45) and (37)

$$0>p^2[J_0(r^{(2)})+J_4(r^{(2)})]^2-4(J_2(r^{(2)}))^2 \ . \tag{B5}$$

One can show analogously to Eq. (B2)

$$x^2[J_0(x)+J_4(x)]=2[(14-x^2)J_2(x)-5xJ_2'(x)] \ . \tag{B6}$$

Using this formula in Eq. (B5) at point $x=r_m^{(2)}$ where the derivative of the second-order Bessel function vanishes we obtain the inequality

$$(r_m^{(2)})^2>7 \ , \tag{B7}$$

which is clearly fulfilled for every case-2 stationary point, see Table I.

[1]B. Yurke, L. W. Rupp, and P. G. Kaminsky, IEEE Trans. Magn. **MAG-23**, 458 (1987).

[2]C. M. Caves, Phys. Rev. D **23**, 1693 (1981).

[3]J. H. Shapiro, IEEE J. Quantum Electron. **QE-21**, 237 (1985).

[4]H. P. Yuen, Phys. Rev. A **29**, 2226 (1976).

[5]J. H. Shapiro, Opt. Lett. **5**, 351 (1980).

[6]P. Russer and F. X. Kaertner, Arch. Elektron. Übertragungstechn. **44**, 216 (1990).

[7]M. J. Collett and C. W. Gardiner, Phys. Rev. A **30**, 1386 (1984).

[8]M. J. Collett and D. F. Walls, Phys. Rev. A **32**, 2887 (1985).

[9]S. Reynaud and A. Heidmann, Opt. Commun. **71**, 209 (1989).

[10]B. Yurke, Phys. Rev. A **29**, 1419 (1984).

[11]C. W. Gardiner and M. J. Collett, Phys. Rev. A **31**, 3761 (1985).

[12]K. E. Cahill and R. J. Glauber, Phys. Rev. **177**, 1857 (1969).

[13]M. Hillery, R. F. O'Connell, M. O. Scully, and E. P. Wigner, Phys. Rep. **106**, 121 (1984).

[14]K. E. Cahill and R. J. Glauber, Phys. Rev. **177**, 1882 (1969).

[15]D. Han, Y. S. Kim, and M. E. Noz, Phys. Rev. A **37**, 807 (1988).

[16]J. Gea-Banacloche, N. Lu, L. M. Pedrotti, S. Prasad, M. O. Scully, and K. Wódkiewicz, Phys. Rev. A **41**, 369 (1990).

[17]B. Yurke, J. Opt. Soc. Am. B **4**, 1551 (1987).